Heliyon 9 (2023) e17080

Contents lists available at ScienceDirect

Heliyon

journal homepage: www.cell.com/heliyon

Natural fulvic acids inhibit non-small-cell lung cancer through the COX-2/PGE2/EP4 axis: In silico and in vivo assessments

Pengfei Xin [a,b,*], Shirui Wang [c], Xin Xu [c], Qingmei Liu [a,b], Caifeng Zhang [d,**]

[a] Department of Stomatology, Shanxi Bethune Hospital, Shanxi Academy of Medical Sciences, Tongji Shanxi Hospital, Third Hospital of Shanxi Medical University, Taiyuan, 030032, China
[b] Tongji Hospital, Tongji Medical College, Huazhong University of Science and Technology, Wuhan, 430030, China
[c] Shanxi Medical University School and Hospital of Stomatology, Taiyuan, 030001, China
[d] Department of Chemistry, Taiyuan Normal University, Humic Acid Engineering and Technology Research Center of Shanxi Province, Jinzhong, 030619, China

ARTICLE INFO

Keywords:
Fulvic acids
Humic acids
Non-small-cell lung cancer
Molecular docking
COX-2
EP4

ABSTRACT

Purpose: Non-small-cell lung cancer (NSCLC) is a major public health concern with a high incidence worldwide. Coal-derived fulvic acids (FAs) contain functional groups in their chemical structures. Overexpression of cyclooxygenases-2 (COX-2), prostaglandin E2 (PGE2), and the PGE2 receptor EP4 subtype (EP4) can have a potential link with the increased tumor incidence and promoted tumor growth and metastasis in NSCLC. This study aimed to assess the biological roles of coal-derived FAs in the growth and development of NSCLC and to elucidate the underlying molecular mechanisms.

Methods: A web-based tool for predicting small-molecule pharmacokinetics (pkCSM) was used to analyze the absorption, distribution, metabolism, excretion, and toxicity (ADMET) properties of FAs. Molecular docking and dynamic simulations were performed to analyze the binding affinities of COX-2 and EP4 to FA. An acute toxicity test and an antitumor study were used to analyze the toxicity and anti-NSCLC effects of FAs. Thirty NSCLC-bearing nude mice were randomly divided into five groups (six mice per group): vehicle control, positive control with 20 mg/kg body weight (BW) 5-fluorouracil, and three treatments with 25, 50, and 100 mg/kg BW FAs. The BW and tumor volume were recorded, and the COX-2, PGE2, and EP4 protein expression were measured and analyzed.

Results: Using the predictive pkCSM algorithm, we found that FA did not cause developmental toxicity. Molecular simulations revealed that COX-2 and EP4 expression was inhibited by FA. An acute toxicity test conformed that the maximum tolerated FAs dose was >3.0 g/kg BW. The

Abbreviations: ADMET, absorption, distribution, metabolism, excretion, and toxicity; BCA, bicinchoninic acid; BW, body weight; COX-2, cyclooxygenase-2; ELISA, enzyme-linked immunosorbent assay; EP, prostaglandin E; EP4, prostaglandin E2 receptor EP4 subtype; FAs, fulvic acids; FBS, fetal bovine serum; FDA, Food and Drug Administration; HRP, horseradish peroxidase; NSAID, nonsteroidal anti-inflammatory drug; NSCLC, non-small-cell lung cancer; PGE2, prostaglandin E2; PMT, photomultiplier tube; RIPA, radioimmunoprecipitation assay; RMSD, root mean square deviation; RMSF, root mean square fluctuations; SDS-PAGE, sodium dodecyl sulfate-polyacrylamide gel electrophoresis; SNK, Student-Newman-Keuls; SPF, specific pathogen free; TBST, tris buffered saline with tween 20; UV-Vis, ultraviolet-visible; WB, western blot.

* Corresponding author. Department of Stomatology, Shanxi Bethune Hospital, Shanxi Academy of Medical Sciences, Tongji Shanxi Hospital, Third Hospital of Shanxi Medical University, Taiyuan, 030032, China.
** Corresponding author.
E-mail addresses: lifesaver@alumni.sjtu.edu.cn (P. Xin), zhangcf301@tynu.edu.cn (C. Zhang).

https://doi.org/10.1016/j.heliyon.2023.e17080
Received 22 November 2022; Received in revised form 6 June 2023; Accepted 7 June 2023
Available online 7 June 2023

animal study demonstrated that FA treatment significantly downregulated the expression of COX-2, PGE2, and EP4 in NSCLC-bearing mice compared to that in vehicle control mice ($p < 0.01$). *Conclusions:* Natural FAs may exert anti-NSCLC effects through the COX-2/PGE2/EP4 axis.

1. Introduction

Lung cancer is one of the most prevalent malignant tumors and has become a significant global public health issue. Lung cancer is the most common cancer type in the USA and China. Based on the statistical data of the American Cancer Society, which shows that lung and bronchial cancer fatalities account for 21% of all cancer deaths, >350 individuals die from lung cancer daily [1]. Lung cancer deaths affect approximately 29.7% of men and 22.9% of women, as reported by the National Cancer Center of China; therefore, it is expected that more people will die from the disease in the future [2].

Non-small-cell lung cancer (NSCLC) and small cell lung cancer are the two main subtypes of lung cancer, with NSCLC accounting for approximately 80%–85% of all cases [3]. Lung cancer should be treated using a strategy that combines multidisciplinary and customized treatments. A planned and logical approach to the use of surgery, radiation, chemotherapy, molecular targeted therapy, and immunotherapy will extend patient survival and enhance quality of life. Chemotherapy, molecular targeted therapy, and immunotherapy are types of drug treatments used against lung cancer [4]. Chemotherapy should consider the disease stage, physical status, adverse reactions, and quality of life of the patient, and providing excessive or insufficient care should be avoided. Gene mutation status must be determined for molecular targeted therapy to guide targeted therapy based on the molecular type. In recent years, it has been demonstrated that immunotherapy in the form of immune checkpoint inhibitors improves the survival rate of patients with lung cancer [5]. Lung cancer therapy has several drawbacks owing to the complexity of tumors, unfavorable medication reactions, drug resistance, and patient variances. Over the past 10 years, the United States Food and Drug Administration (FDA) has approved approximately 20 new targeted medicines, but further innovative agents still require evaluation [6]. Therefore, it is necessary to identify additional disease targets and develop novel therapeutic drugs.

Cyclooxygenase-2 (COX-2) expression is negligible in most normal cells and can be upregulated and overexpressed in cells only in inflammatory or tumorigenic environments [7,8]. COX-2 is a crucial enzyme involved in the production of prostaglandins and is significantly expressed in a range of malignant tumors and precancerous lesions [9–11]. Its metabolites are processed by several downstream prostaglandin synthetases to produce various bioactive prostaglandins such as prostaglandin E2 (PGE2). COX-2 and PGE2 are important in chronic inflammatory diseases and can enhance the incidence of tumors as well as their growth and metastasis [12]. The immunosuppressive network in the pathogenesis of NSCLC, including tumor proliferation, invasion, angiogenesis, and resistance to apoptosis, is driven by high expression levels of COX-2 and its product PGE2 [13,14]. In human NSCLC cells, PGE2 enhances tumor progression by promoting cancer cell proliferation and invasion, and by producing a microenvironment that supports tumor growth [15]. Previous studies have shown that mitogens, cytokines, and tumor promoters can enhance the expression of the COX-2 isoform in lung adenocarcinomas, and COX-2/PGE2 overexpression has been linked to NSCLC [14–16]. Therefore, decreased COX-2 expression may be able to treat NSCLC.

PGE2 binds to different prostaglandin E2 receptors to activate specific downstream signaling pathways, including the β-catenin, PKA, NF-κB, and PI3K/AKT pathways, which are all crucial for the biological and pathological behavior of the tumor. PGE2 receptors contain G protein-coupled receptors on the cell surface, known as prostaglandin E (EP) receptors; four different receptors have been identified and designated as EP1, EP2, EP3, and EP4 [12]. Compared with other EP receptors, the function of EP4 receptors in malignancies is better understood. EP4, a high-affinity EP receptor, is hypothesized to function as a pro-cancer mediator in several malignancies owing to its high expression. EP4 receptor signaling is particularly important for tumor angiogenesis, proliferation, and migration [17]. The various biological functions of EP4 in the development of cancer are connected to distinct signaling pathways that EP4 may activate [17,18]. An in vivo study reported that the suppression of EP4 in a mouse model prevented oral cancer cells from spreading to the lungs [19]. However, cell studies have shown that reduced EP4 protein levels limit the proliferation of NSCLC cells [20,21]. Moreover, selective EP4 antagonists, which block signaling pathways mediated by the EP4 receptor, may be effective cancer treatments [20,22].

Therefore, it appears that the COX-2/PGE2/EP4 signaling pathway is essential for the growth of malignancies, and it may be beneficial to develop drugs that block this axis [23,24].

Humic acids (HAs) are weak macromolecular organic acid mixtures that occur naturally due to a complex series of geochemical and biological processes involving dead animal and plant remains [25]. Quinones, phenols, and carboxylic acids are some of the functional groups found in the chemical structures of HAs, and they have indeterminate compositions that change depending on the source and method of production [26]. In the "Compendium of Materia Medica" of Li Shizhen, which was originally written during the Ming Dynasty, *wujinshi* was identified as a traditional Chinese medication, and HAs were principally responsible for its pharmacological effects [27]. *Wujinshi* was historically used to heal knife wounds, promote the elimination of gold, silver, and coins from the abdomen, treat menstrual disorders, and relieve postpartum abdominal pain, based on the records of the "Compendium of Materia Medica". HAs can be used to accelerate wound healing [28,29] and function as antiviral agents [30]. Fulvic acids (FAs), one of the three HAs fractions, differ from black HAs and hymatomelanic acids in that they have a smaller molecular weight, greater solubility, and greater biological activity [31]. FAs are primarily derived from weathered coal, peat, and young lignite. Because of their strong water solubility and ability to be easily absorbed by organisms, FAs are typically used in mixtures. FAs are thought to be a potentially risk-free natural active component of HAs and appear a good candidate to be further explored as a functional excipient [32,33]. However, the

chemical compositions of FA are not yet fully understood. Currently, a proven unit in the FA component is a substance with the molecular formula $C_{14}H_{12}O_8$; its structure can be retrieved from the PubChem database (https://pubchem.ncbi.nlm.nih.gov, PubChem CID:5359407).

In vitro cell studies have revealed that FAs have antitumor capabilities [34,35]. However, reports on the in vivo anticancer effects of FAs are scarce. Molecular docking was used to mimic the binding of FA to the target protein before starting the animal study reported here. Drug design using molecular docking is based on the properties of the receptors and their interactions with medicinal molecules. This technique primarily uses theoretical modeling to examine how molecules (such as ligands and receptors) interact and predict their binding affinities. Similar to the molecular docking method, a previous study investigating naphthoquinone derivatives as potential anticancer candidates found that compound 16 interacted with COX-2 at the arachidonic acid site [36]. As a result, this study began with a molecular docking simulation of FA with COX-2 and EP4 and then designed an in vivo study for validation.

This study aimed to assess the biological roles of coal-derived FAs in the growth and development of NSCLC and to elucidate the underlying molecular mechanisms.

2. Materials and methods

2.1. Absorption, distribution, metabolism, excretion, and toxicity (ADMET) prediction

The ADMET approach is essential for drug development and screening. In addition to effectively resolving the issue of species differences, the evaluation of ADMET properties in the early stages of drug development can significantly increase the success rate of drug research and development, lower the cost of drug development, and decrease the occurrence of drug toxicity and side effects. The two-dimensional (2D) structure/SMILES of the FA molecules were obtained from the PubChem database. To calculate the ADMET properties of FA, the web-based tool for predicting small-molecule pharmacokinetics pkCSM (http://biosig.unimelb.edu.au/pkcsm/prediction) was used. This machine-learning platform uses graph-based signatures to build predictive models of key ADMET properties for drug development [37]. It consists of 28 regression and classification models tested and trained on various experimental datasets, including a wide range of ADMET descriptors. The 2D structure/SMILES of FA was used as the keyword to be retrieved from pkCSM.

2.2. Molecular docking and molecular dynamics simulations

COX-2 and EP4 protein structure files were retrieved from the Protein Crystal Database protein data bank (PDB; http://www.pdb.org/). FA was selected as the ligand, and COX-2 and EP4 were selected as receptors. Celecoxib is a non-steroidal anti-inflammatory drug (NSAID) that selectively inhibits COX-2, and grapiprant is an orally bioavailable EP4 antagonist. The molecular structures of PGE2, celecoxib, and grapiprant with known functions, were obtained from PubChem. They were used as controls to determine the extent to which FA bound to the two proteins. Molecular docking and binding affinity calculations were completed using AutoDock Vina software (version 1.2.0) [38].

The drug small molecule docked by the Vina calculation was inserted into the macromolecule file after opening the protein macromolecule in BIOVIA Discovery Studio (version 4.5, Dassault Systèmes, France) program. To create a receptor-ligand complex, we selected the drug small-molecule chain and drag it into the protein macromolecule. Subsequently, a standard dynamic cascade was performed. A cubic simulation box was used to contain the ligand-receptor complex solvated with explicit periodic boundary constraints. The counterion of the simulation was set at a salt concentration of 0.145 NaCl, and the CHARMM force field was then applied to the system.

The system was subjected to the following simulation protocols: 1000-step minimization through steepest descent and conjugate gradient, 20-ps ensemble equilibration simulations at a temperature of 300 K, and 200-ps production simulation at a temperature and pressure that were both normal. The time step of the simulation system was set to 2.0 fs. A trajectory was calculated for the root mean square deviation (RMSD), root mean square fluctuation (RMSF), and potential energy using celecoxib/grapiprant/PGE2 settings as references.

2.3. FA preparation and characterization

FAs (No. HFS-ZCF341) was obtained from the Humic Acid Engineering and Technology Research Center of Shanxi Province and was extracted from Inner Mongolian lignite using the hydrogen peroxide method. The mineral FA content was determined according to the national standard of the People's Republic of China (GB/T 34765-2017). The FAs content was >90%, and the heavy metal content was ≤50 mg/kg. FA (0.5g) was added to 1 L of purified water and diluted to 50 mg/L for subsequent experiments.

2.3.1. Ultimate analysis and ultraviolet–visible (UV–Vis) spectrum

The concentrations of C, H, O, N, and S in the FAs were examined, and the molar ratio of each atom was calculated using an elemental analyzer (vario EL cube, Elementar, Germany). The FA sample was placed in a sample cell made of fused quartz glass with an optical path length of 10 mm and used to evaluate the absorbance of the sample using a UV–Vis spectrophotometer (TU-1902, Puxi General Instrument Co., Ltd., Beijing) at 20–25 °C. Deionized water was used as the blank control, and the wavelengths were set at A465 and A665 nm (for E4 and E6, respectively). Absorption values were measured to determine the E4/E6 ratio.

2.3.2. Fluorescence spectrum

The FA sample was transferred into a 1 cm cuvette, and the fluorescence spectrum was scanned using a Cary Eclipse fluorescence spectrophotometer (VARIAN Company, USA). The emission spectrum was repeatedly scanned using various excitation wavelengths and the excitation spectrum was scanned using the emission wavelength that produced the highest intensity. The fluorescence peak was identified as the group with the highest excitation and emission intensities and matching. The fundamental functional criteria were as follows: Xenon flash lamp, photomultiplier tube (PMT) voltage of 600 V, excitation and emission slits of 5 nm, scanning speed of 600 nm/min, average time of 0.1000 s, and a data interval of 1.0000 nm.

2.4. Laboratory animals

Animal studies include acute FA toxicity tests and antitumor studies. Forty specific pathogen-free (SPF) Institute of Cancer Research (ICR) mice (20 males and 20 females) were used for the acute toxicity test. Thirty BALB/c nude mice (all male) were used for the in vivo antitumor study. Mice were obtained from Charles River (Beijing) Co., Ltd. and reared in a barrier environment. All procedures were conducted in accordance with the National Research Council's Guide for the Care and Use of Laboratory Animals and were approved by the Laboratory Animal Ethics and Welfare Committee of Shanxi Bethune Hospital at the Shanxi Academy of Medical Science (SBQDL-2022-067).

2.5. Acute toxicity test

Forty ICR mice were fasted for 16 h with free access to water and randomly divided into control (purified water) and FA groups based on their body weight (BW), with 20 mice in each group (10 males and 10 females). The maximum dosage method was adopted, and the FA group was given FA by gavage with a drug concentration of 0.10 g/mL and a drug volume of 3 mL/100 g. Equal volumes of purified water were administered to the control group. The toxic reactions and death of the animals after administration for 14 d were observed and recorded. Animals were weighed before administration and 1, 3, 8, and 14 d after administration, and animal feed consumption was determined at 3 and 10 d after administration.

Toxicity symptoms and death of the animals were observed after administration. All animals were observed twice daily (in the morning and afternoon) for the first 3 d after administration and once daily in the morning for the next 11 d, for a total of 14 d. The toxicity symptoms of the animals, including the starting time, severity, and duration, as well as death of animals, were recorded. Animals that died during the study, as well as all animals that had been anesthetized with pentobarbital sodium at the end of the study, were subjected to gross autopsies. Major organs and tissues, including the heart, liver, spleen, lung, kidney, gastrointestinal system, were examined.

2.6. Antitumor study

2.6.1. Establishment of a tumor-bearing nude mouse model

Cell culture conditions were as follows: Human NSCLC A549 cells were obtained from the Cell Bank of the Chinese Academy of Sciences (Shanghai, China). The cells were maintained in F12–K (Gibco, US) medium supplemented with 10% fetal bovine serum (FBS; Gibco, US) and 1% penicillin-streptomycin (Gibco, US) at 37 °C in a humidified incubator with 5% CO2. The medium was changed every other day, and the cells were passaged at a ratio of 1:3 every 3 d. When the cells grew adherently and reached 95% of the bottom of the flask, the culture medium was discarded, and the cells were harvested after segregating with 0.25% trypsin (Gibco, US).

The A549 cells were washed with normal saline before being diluted to obtain a cell suspension of 1×10^7 cells/mL. Cells (0.2 mL) were inoculated subcutaneously into the middle of the axilla of each nude mouse, and the number of inoculated tumor cells was 2×10^6. After inoculation, the animals were raised in a barrier environment and the tumor volume was measured every 3–4 d. When the tumor volume of the animals reached approximately 100 mm^3, they were randomly divided into five groups for follow-up experiments.

2.6.2. Organization and grouping

FA (0.5g) was added to 50 mL of purified water to prepare a 1% solution (10 mg/mL) and diluted to prepare 5 mg/mL and 2.5 mg/mL FA solutions.

Thirty A549-bearing nude mice were established and randomly divided into five groups (six mice per group): vehicle group (purified water), FA25 group (FAs = 25 mg/kg BW), FA50 group (FAs = 50 mg/kg BW), FA100 group (FAs = 100 mg/kg BW); and positive group (5-fluorouracil (Sigma; St. Louis, MO, USA) = 20 mg/kg BW). On the day of grouping, the vehicle and FAs groups were all administered through gavage, with a dose of 0.1 mL/10 g BW administered once daily for 4 weeks. Mice in the positive group were intraperitoneally injected with 5-fluorouracil twice weekly.

2.6.3. Effect of FA on BW and tumor growth

Throughout the investigation, weekly measurements and BW of the animals were recorded. Tumor volumes were measured twice weekly. Tumor diameter was measured using a Vernier caliper. The maximum perpendicular diameter was recorded as a, and the minimum perpendicular diameter was recorded as b. The tumor volume was calculated as $v = 0.5a \times b^2$, where a and b are the maximum and minimum diameters, respectively [39]. Pentobarbital sodium was used to induce anesthesia in all animals at the end of the study and blood was drawn from the eye sockets. The mice were sacrificed through cervical dislocation. Tumors were excised, weighed, volumetrically measured, and analyzed.

2.6.4. Protein expression of the COX-2/PGE2/EP4 axis

Blood samples were collected and placed in clean ethylenediaminetetraacetic acid (EDTA) anticoagulation tubes. After centrifugation at 3000*g* for 5 min, the serum supernatant was collected. The serum PGE2 levels in each group were estimated using an enzyme-linked immunosorbent assay (ELISA) kit from Labsystems Multiskan MS Type 352 Microplate Reader (Finland). The Mouse PGE2 ELISA kit was purchased from Andygene (Guangdong, China).

Radioimmunoprecipitation assay buffer (RIPA; Servicebio, China) was used to lyse the tumor tissue for total protein extraction. The homogenates were then centrifuged at 12000 *g* for 20 min at 4 °C, and the supernatants were preserved as protein samples at −80 °C until further use. The protein concentration was determined using a bicinchoninic acid (BCA) protein assay kit (Servicebio, China). The samples were subjected to 10% sodium dodecyl sulfate-polyacrylamide gel electrophoresis (SDS-PAGE; Servicebio, China) and then transferred to polyvinylidene fluoride (PVDF) membranes (Servicebio, China). The membranes were blocked in 5% nonfat milk (Servicebio, China) in Tris Buffered Saline with Tween 20 (TBST; Servicebio, China) for 1 h at room temperature and incubated with the primary antibodies against COX-2 (Servicebio, China), EP4 (Cohesion, UK), and β-Actin (Servicebio, China) overnight at 4 °C. Membranes were washed thrice with TBST after overnight incubation and then incubated with a goat anti-rabbit horseradish peroxidase (HRP)-conjugated secondary antibody (Servicebio, China) at room temperature for 1 h. The protein density was measured using a ChemiScope Imaging System (6100; Clinx, China). Western blots (WB) were quantified using ImageJ software (1.53t; NIH, Bethesda, MD, USA).

2.7. Statistical analysis

SPSS statistics software (version 26, IBM Corp., USA) was used for statistical analysis and drawing. In the acute toxicity test, the results of measured BW and feed consumption data were expressed as the mean value ± standard deviation (SD), and a paired *t*-test was conducted. The results of weight gain, and tumor volume in an antitumor study were expressed as the mean value ± SD ($\bar{x}\pm s$). One-way analysis of variance (ANOVA) test followed by post hoc Student-Newman-Keuls (SNK) multiple comparisons test was used to compare the differences among groups, with statistical significance set at $p < 0.05$.

3. Results

3.1. ADMET prediction

pkCSM is a web-based tool used to analyze the pharmacokinetic properties of a selected compound. Based on the predictive pkCSM algorithm, FA did not cause developmental toxicity (Table 1).

3.2. Analysis of receptor-ligand binding

The interactions of COX-2 and EP4 with the appropriate active substances were determined using AutoDock Vina. The free binding affinities of the proteins to the active substances are shown in Table 2. Both hydrogen bonds and van der Waals forces play a role in the binding affinity. Hydrogen bond formation is facilitated by the functional groups of FAs with the oxygen, hydroxyl, carbonyl, and carboxyl groups. Carbonyl groups and oxygen-containing rings can accept hydrogen, whereas hydroxyl groups can only offer hydrogen. The results showed that FA could interact with COX-2 and EP4 through hydrogen bonds, π-related interactions, and other interactions. The binding affinities were slightly weaker than those of the control compounds, suggesting that FA may have a more reversible ability and fewer adverse effects.

Table 1
ADMET (Absorption, Distribution, Metabolism, Excretion, and Toxicity) properties of fulvic acid (FA) predicted by pkCSM.

Property	Model name	Predicted value	Interpretation
Absorption	Intestinal absorption (human)	48.397% Absorbed	<30% is considered to be poorly absorbed.
	Skin Permeability	−2.735 log Kp	logKp > −2.5 is considered to have a relatively low skin permeability
Distribution	VDss (human)	0.039 log L/kg	It is considered low if < 0.71 L/kg (log VDss < −0.15) and high if > 2.81 L/kg (log VDss >0.45)
	BBB permeability	−1.149	A logBB >0.3 considered to readily cross the blood-brain barrier, whereas molecules with logBB < −1 are poorly distributed to the brain
Metabolism	CYP2D6 substrate	No	Noninhibitor of cytochrome P450
Excretion	Total Clearance	0.501 log mL/min/kg	–
	Renal OCT2 substrate	No	Not likely to be an OCT2 substrate
Toxicity	Hepatotoxicity	No	–
	Skin Sensitisation	No	–
	hERG I and II Inhibitors	No	Not likely to be a hERG I/II inhibitor
	MTD (human)	0.802 log mg/kg/d	A MTD of ≤0.477 log (mg/kg/day) is considered low, and high if > 0.477 log (mg/kg/d).

VDss, volume of distribution; BBB, blood-brain barrier; BB, blood-brain; CYP2D6, cytochrome P450 family 2 subfamily D member 6; OCT2, organic cation transporter 2; hERG, human ether-a-go-go related gene; MTD, maximum tolerated dose.

Table 2
Molecular docking information.

Compounds	Binding Affinity (kcal/mol)	
	COX-2 (PDB ID:5F1A)	EP4 (PDB ID:5YWY)
Fulvic acid (PubChem CID:5359407)	−8.411	−7.553
Grapiprant (PubChem CID:11677589)	–	−9.354
PGE2 (PubChem CID:5280360)	–	−7.813
Celecoxib (PubChem CID:2662)	−9.160	–
5-fluorouracil (PubChem CID:3385)	−5.778[a]	−5.135[a]

[a] It is possible that the predicted binding site is inconsistent with the actual binding pocket, and that the calculated binding affinity is too weak to be reliable.

Celecoxib was an inhibitor of COX-2 with a binding affinity of −9.160 kcal/mol. The binding affinity of FA to COX-2 was slightly weaker than that of celecoxib to COX-2 (−8.41 kcal/mol). Both celecoxib and FA established conventional hydrogen bonds with specific Tyr385 residues and interacted with Gln203 and Trp387 residues through molecular forces, such as hydrogen bonds and hydrophobic interactions (Fig. 1A and B).

EP4 was inhibited by grapiprant, with a binding affinity of −9.353 kcal/mol, and PGE2 was agonistic to EP4, with a binding affinity of −7.813 kcal/mol. FA had a binding affinity of −7.553 kcal/mol to EP4, which was slightly weaker than the binding affinity of grapiprant or PGE2 to EP4. The Ser319 and Arg106 residues of EP4 formed conventional hydrogen bonds with FA or the inhibitor grapiprant as well as a carbon-hydrogen bond with the Thr69 residues. PGE2, an agonist, formed hydrogen bonds with EP4 residues Pro24 and Cys170, as well as carbon-hydrogen bonds with Ser95 and Trp169 (Fig. 2A–C). Compared to grapiprant and FA, the binding

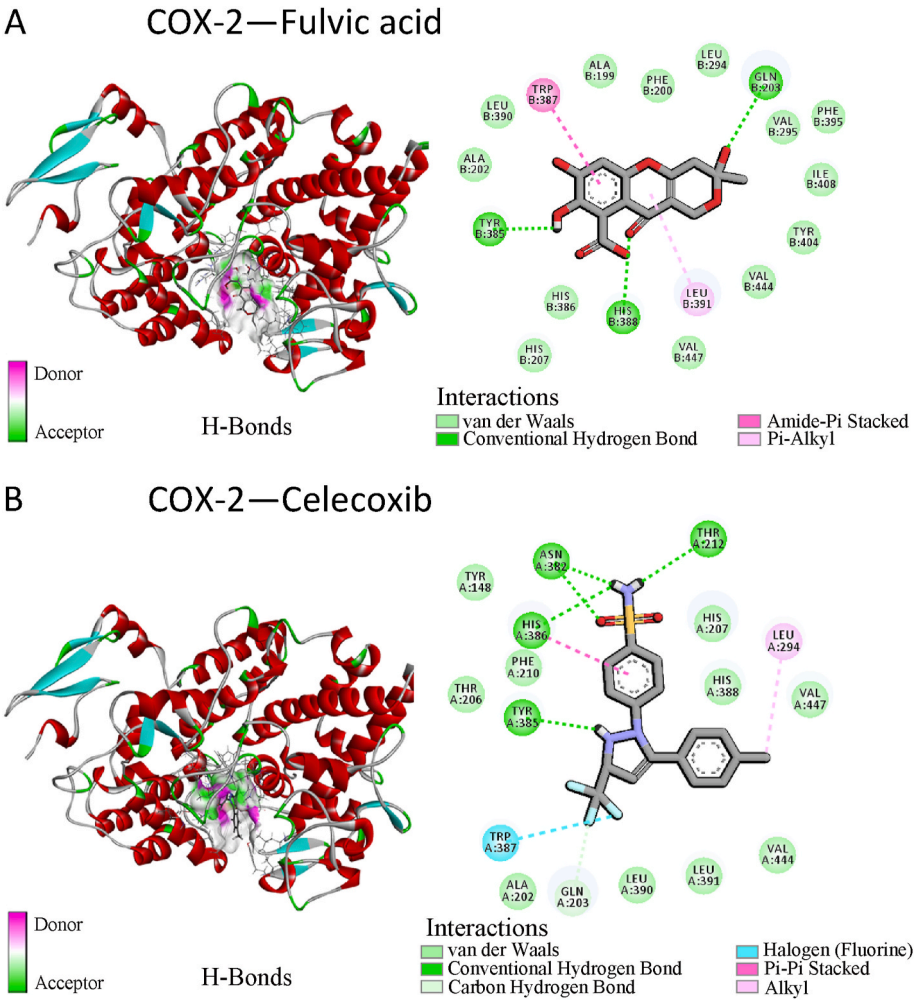

Fig. 1. Schematic representation of the molecular docking models of cyclooxygenase-2 (COX-2) binding with fulvic acid (FA) (A) and celecoxib (control, an inhibitor of COX-2) (B).

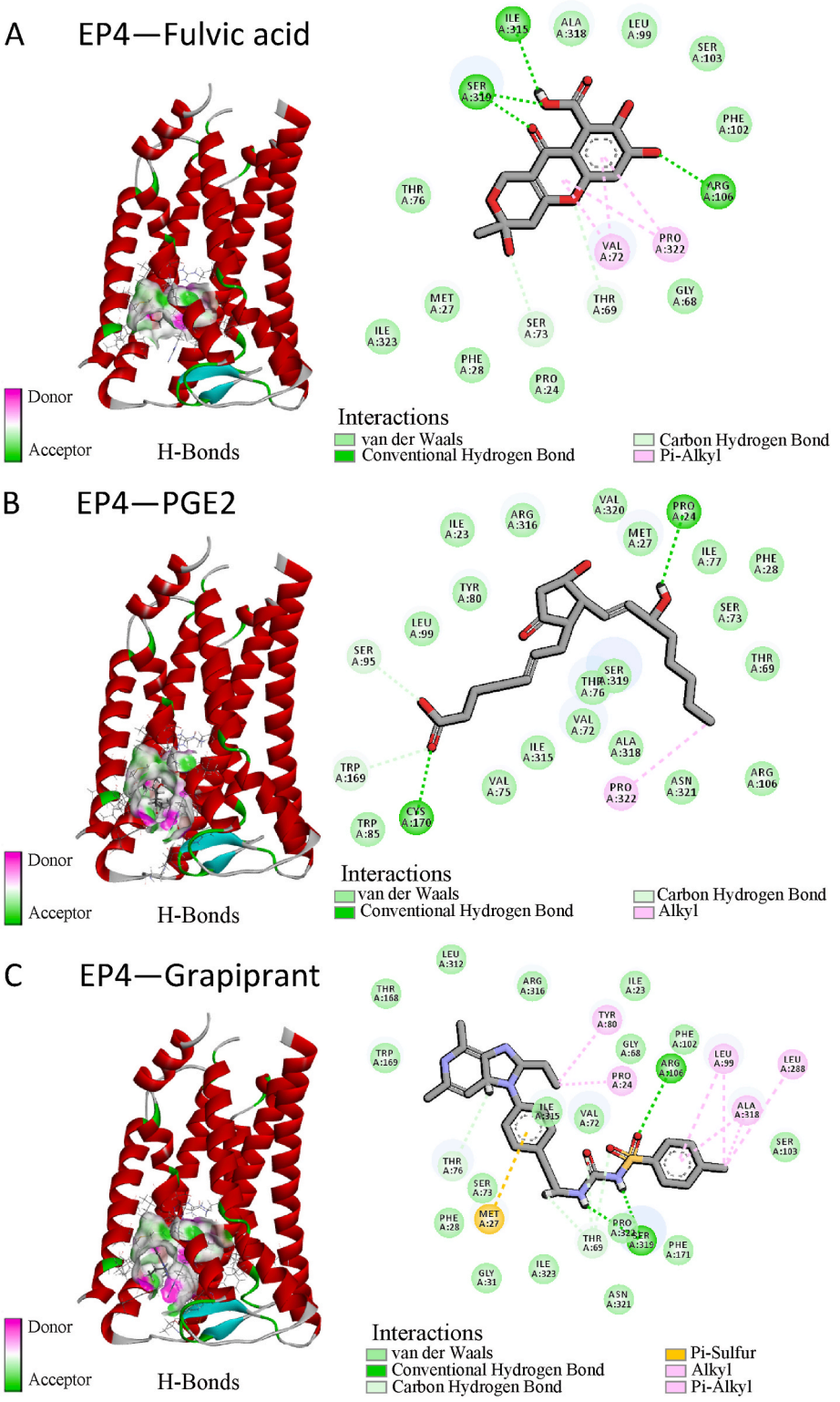

Fig. 2. Schematic representation of the molecular docking models of prostaglandin E2 (PGE2) receptor EP4 subtype (EP4) binding with FA (A), PGE2 (control, an agonist of EP4) (B), and grapiprant (control, an inhibitor of EP4) (C), respectively.

sites of these amino acid residues on PGE2 differed.

Molecular docking revealed that 5-fluorouracil had poor binding energy to COX-2 and EP4, and that its binding site was different from how these two proteins interacted with natural ligands; the simulation results of 5-fluorouracil binding to these two proteins were unreliable (Table 2 and Fig. 3A–D).

The results of AutoDock Vina were used to run molecular dynamic simulations using the Standard Dynamics Cascade module of Discovery Studio software. After a certain period, the RMSD, RMSF, and potential energies of these complexes reached a relatively stable and balanced state (Fig. 4A–F). Based on the molecular docking simulations and molecular dynamics equilibrated trajectories, FA has the same ability as celecoxib and grapiprant to block the entrance of the catalytic substrate to the reactive domains of COX-2 and EP4, respectively.

3.3. Ultimate analysis, UV–Vis, and fluorescence spectrum of FAs

FAs mostly contained the elements C, O, H, N, and S, with C accounting for 48.42% of the total, O for 16.61%, H for 3.06%, N for 1.20%, and S for 3.29%. H/C and O/C were calculated to have atomic molar ratios of 0.76 and 0.26, respectively. The absorbance values of FA at 465 nm and 665 nm were 0.162 and 0.032, respectively, based on the UV–Vis spectrum, whereas the E4/E6 ratio was 5.06 at both wavelengths. The fluorescence spectrum revealed that FAs exhibited one emission peak at 531 nm and two excitation peaks at 367 and 459 nm, respectively (Fig. 5A).

3.4. Acute toxicity test

There were no clear abnormalities in either the FA or control groups. At 30 min, 6 h, 24 h, 48 h, 7 d, and 14 d, there were no deaths, drowsiness, sedation, skin changes, pains, or convulsions. There was no noticeable difference in BW between the FA and control groups on days −1, 1, 3, 8, and 14. (Table 3 and Fig. 5B). There was no discernible difference between the feed consumption of the two groups on days 3 and 10 ($p > 0.05$). After the study, all animals in both groups were dissected and examined. The subcutaneous and major organs are positioned, shaped, and colored as they would normally be in the thoracic and abdominal chambers. The gastrointestinal

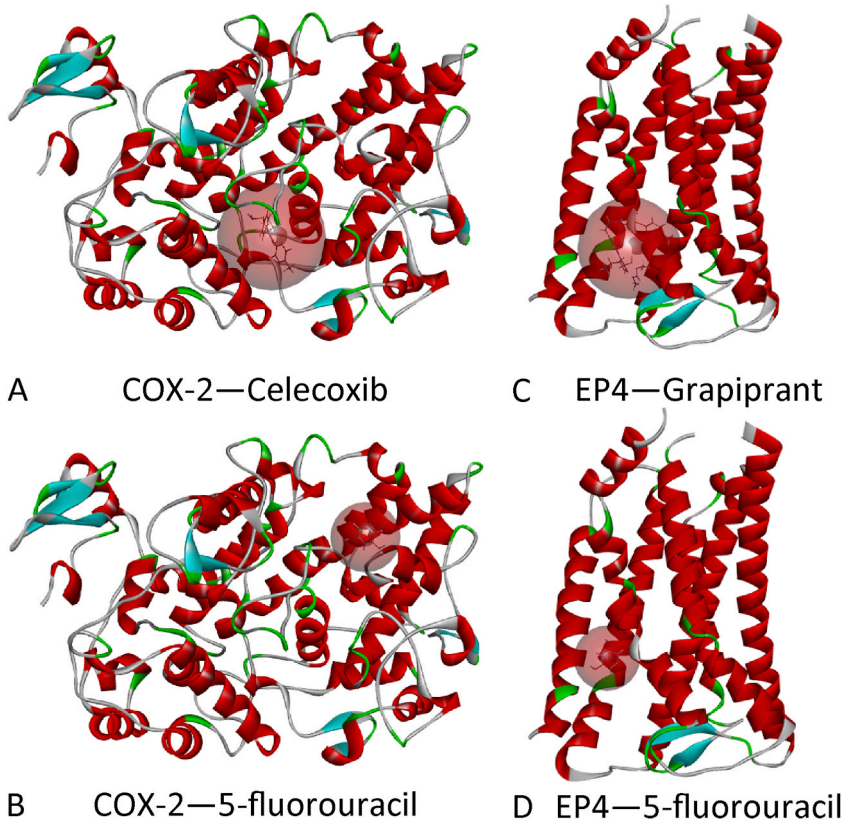

Fig. 3. Molecular docking models of COX-2 binding with celecoxib (A) and 5-fluorouracil (B), and EP4 and grapiprant (C) and 5-fluorouracil (D). The red spheroid illustrating the binding pocket of the receptor implies that the simulated binding site of the 5-fluorouracil does not match the natural one (celecoxib or grapiprant). (For interpretation of the references to color in this figure legend, the reader is referred to the Web version of this article.)

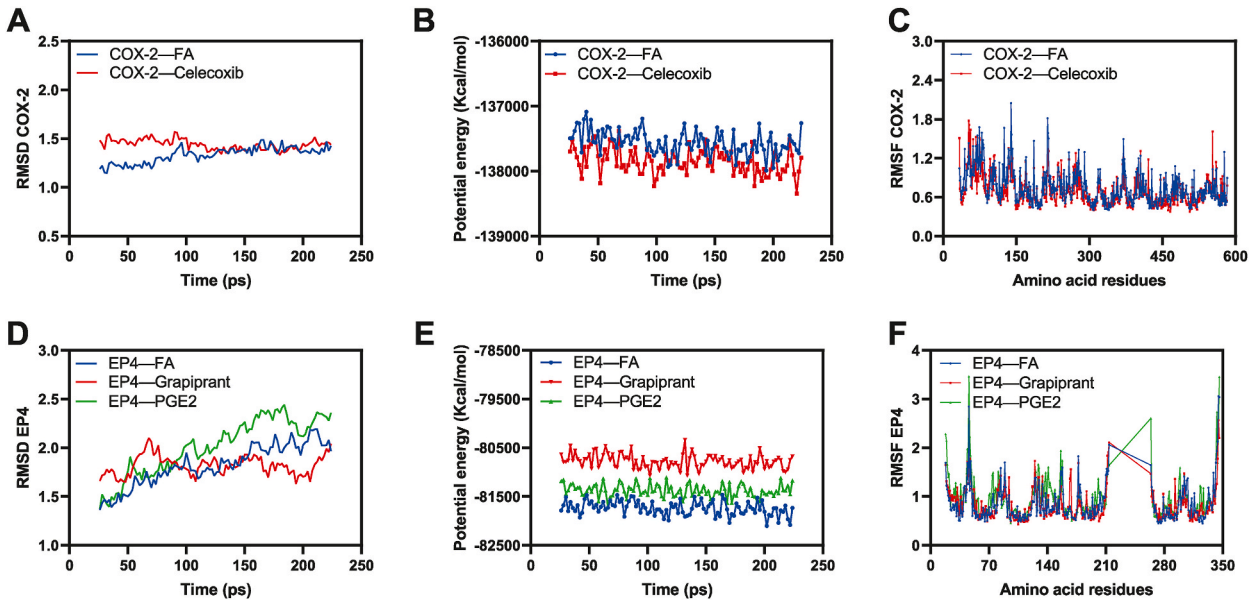

Fig. 4. Diagrammatic exhibition of molecular dynamics simulation: (A) Root Mean Square Deviation (RMSD) of COX-2, (B) Potential Energy of COX-2, (C) Root Mean Square Fluctuations (RMSF) of COX-2 amino acids, (D) RMSD of EP4, (E) Potential Energy of EP4, and (F) RMSF of EP4 amino acids.

tract, lungs, kidneys, livers, and other organs are healthy. The gavaged FA dose that was maximally tolerated for ICR mice during this study was greater than 3.0 g/kg BW.

3.5. Antitumor study

On day 3 after receiving the A549 tumor cell injection, all tumor-bearing nude mice displayed visible tumor tissues beneath the skin on the central and lateral axillary sides. No mice perished spontaneously during the study. The weight gain, tumor weight, and tumor volume in each group at the end of the study are shown in Table 4. The results showed that FA had no impact on the BW of tumor-bearing mice, whereas mice treated with 5-fluorouracil suffered anorexia and lost more weight than mice in the other groups (Fig. 5C).

The volume of mouse tumors increased over time in each group, but the FAs and 5-fluorouracil group tumors decreased compared to the vehicle group (Fig. 5D). Although the weight gain of the 5-fluorouracil mice was significantly greater than that of the vehicle group, the weight gain of the FAs mice was not significant compared to that of the vehicle group (Fig. 5E). After the tumor tissues were removed from the mice at the conclusion of the study, the tumor weights of the FA and the 5-fluorouracil groups (Fig. 5F) and tumor volumes (Fig. 5G) were significantly different from those of the vehicle group. Only the tumor volume of the FA100 group in this study was significantly lower than that of the other observation groups; however, clinically, there was no difference in tumor volume and weight between the FAs and 5-fluorouracil groups.

ELISA results demonstrated that FA decreased serum PGE2 levels in A549 tumor-bearing mice and that the FA100 group had lower PGE2 levels than the FA25 and FA50 groups (Fig. 6A). WB findings showed that COX-2 and EP4 protein expression in the tumor tissues of FA25, FA50, and FA100 mice was significantly lower than that in the vehicle group ($P < 0.01$) (Fig. 6B–D, Supplementary Material, Fig. S1). The FA100 group showed the lowest COX-2 protein expression, which was notably lower than that of the 5-fluorouracil group.

4. Discussion

Drug safety is the most important consideration when developing new medicines. Oral administration of FAs at 5000 mg/kg BW/day to ICR mice or Sprague-Dawley (SD) rats did not result in any deaths or harmful effects, based on both acute toxicity and 60-d sub-chronic toxicity studies [32]. Following a 90-d exposure to FAs, another oral toxicity trial found no general or organ toxicity, and no observable adverse effects were found at 2000 mg/kg BW/d in Wistar rats [40]. In a previous study, the addition FAs or HAs did not significantly affect feed intake, weight gain, or feed conversion ratio [41]. The results of these studies are identical to those of the present study. According to some academics, the oral administration of FAs appears to be safe, and they recommend that it be further investigated for use in food as a functional excipient or nutritional supplement [33,42].

Binding site (pocket) and binding affinity (energy) are the main factors in molecular docking. These factors both affect how accurately the software predicts the receptor-ligand binding. This binding can be performed reliably if the predicted binding site agrees with the actual binding site of the receptor and ligand, as seen using X-ray diffraction (XRD). Otherwise, predicted binding may be unreliable.

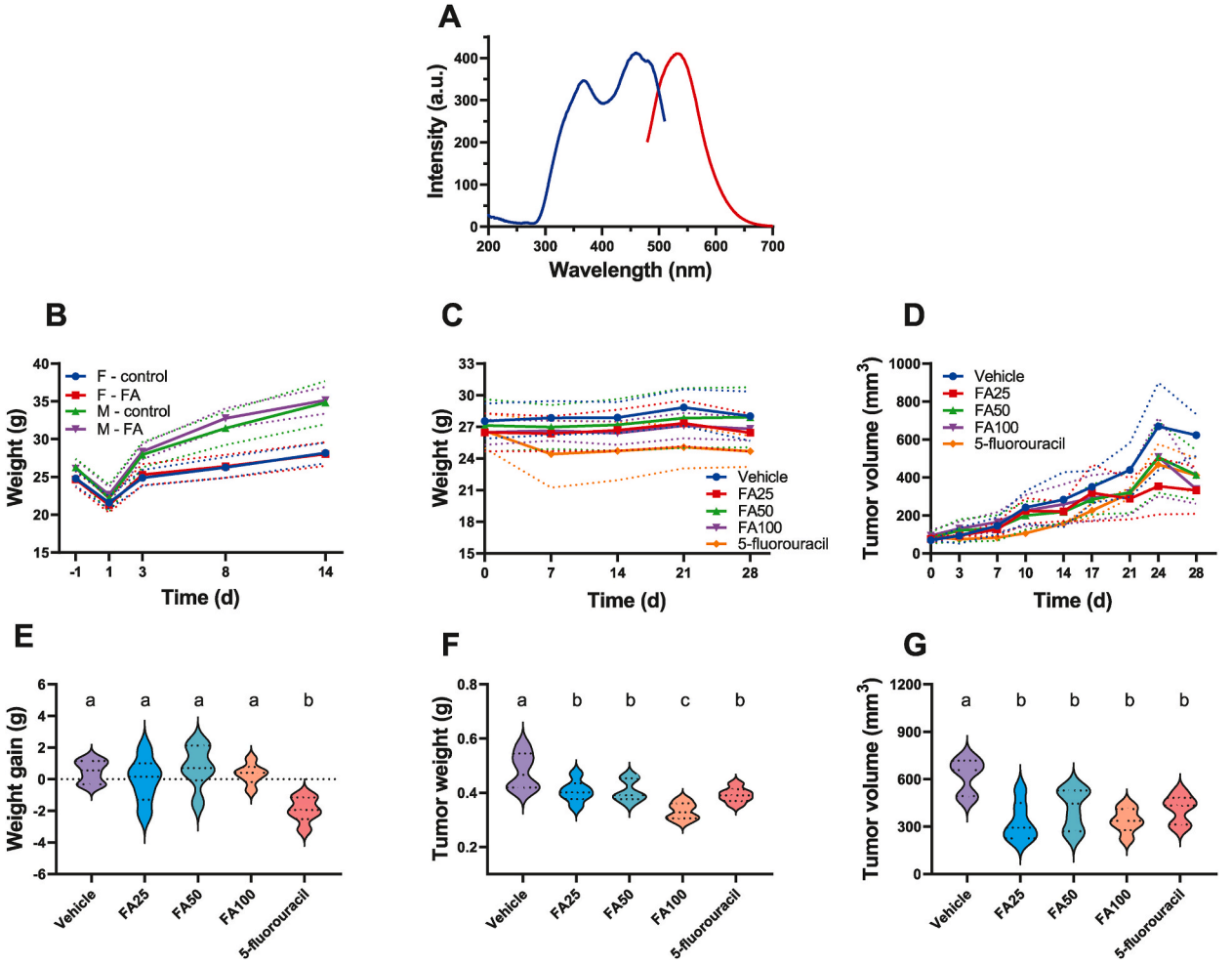

Fig. 5. Characterization of FAs and the animal studies.(A) Fluorescence spectrum of FAs, (B) a trend diagram showing the body weight changes in male ($p = 0.1136$) and female mice ($p = 0.989$) in the acute toxicity test of FAs (paired *t*-test, $n = 20$), (C) weight changes in the anti-tumor study ($p = 0.003$, one-way analysis of variance [ANOVA], $n = 30$, hereinafter same), (D) growth and changes in tumor volume in each group ($p = 0.022$), (E) a comparison of the mean weight gain in each group with that of the other groups at the end of the antitumor study ($p < 0.001$), (F) tumor weight and (G) tumor volume comparison at the end of the antitumor study ($p < 0.001$, respectively). Note: Means not sharing any lowercase letters are significantly different by the Student-Newman-Keuls (SNK) test at the 5% level of significance.

Table 3
Weight and feed consumption of the control/FA group for gastric administration in ICR mice ($\bar{x} \pm s$) (total $n = 40$).

Gender	Group	Dosage (g/kg)	n	Weight (g) day					Feed consumption (g) day	
				−1	1	3	8	14	3	10
Female	Control	0	10	24.8 ± 1.0	21.6 ± 0.8	24.9 ± 1.0	26.3 ± 1.4	28.1 ± 1.4	6.7 ± 0.4	6.0 ± 0.3
	FA	3		24.7 ± 1.0	21.3 ± 1.0	25.3 ± 1.4	26.4 ± 1.5	28.0 ± 1.6	6.6 ± 0.1	6.7 ± 0.5
Male	Control	0	10	26.3 ± 1.2	22.2 ± 1.8	27.9 ± 1.7	31.5 ± 2.2	34.8 ± 2.9	5.5 ± 1.2	4.6 ± 0.4
	FA	3		26.1 ± 1.2	22.7 ± 1.0	28.4 ± 1.0	32.8 ± 1.3	35.2 ± 1.8	5.8 ± 0.4	4.8 ± 0.1

Note. There were no significant differences between the FA and the control groups ($p > 0.05$).

According to the "lock and key principle" and the "induced-fit" theory, only when the geometry of the protein (lock) was an exact compliment of that of the substance (key) could the recognition take place and subsequently trigger the catalytic reactions [43]. With a shape and electrostatic distribution that is compatible with (complementary to) the pocket and sufficient or strong interaction to maintain, ligand molecules can be properly integrated into the protein pocket. Molecular docking of FA with COX-2 and EP4 revealed that several hydrogen bonds were formed, and hydrophobic interactions were common. The potential energy of hydrogen bonds significantly impacts drug design and development [44]. With the receptor protein, the aromatic ring structure of the FAs may form a π-bond. These are essential to guarantee that FA interact with specific biological target molecules and activate (or block) their

Table 4
Effects of FA on body weight gain and tumor growth of A549 tumor-bearing nude mice ($\bar{x} \pm s$) (total n = 30).

Group	Dosage	Weight gain	Tumor weight	Tumor volume
	mg/kg	g	g	mm^3
Vehicle	–	0.47 ± 0.72^a	0.48 ± 0.07^a	622.7 ± 109.9^a
FA25	25	-0.05 ± 1.42^a	0.41 ± 0.04^b	331.9 ± 123.5^b
FA50	50	0.77 ± 1.36^a	0.41 ± 0.04^b	412.9 ± 130.0^b
FA100	100	0.33 ± 0.66^a	0.33 ± 0.03^c	338.6 ± 78.0^b
5-fluorouracil	20	-1.9 ± 0.80^b	0.39 ± 0.03^b	411.4 ± 89.0^b

Note. Means not sharing any lowercase letters are significantly different by the Student-Newman-Keuls test at the 5% level of significance.

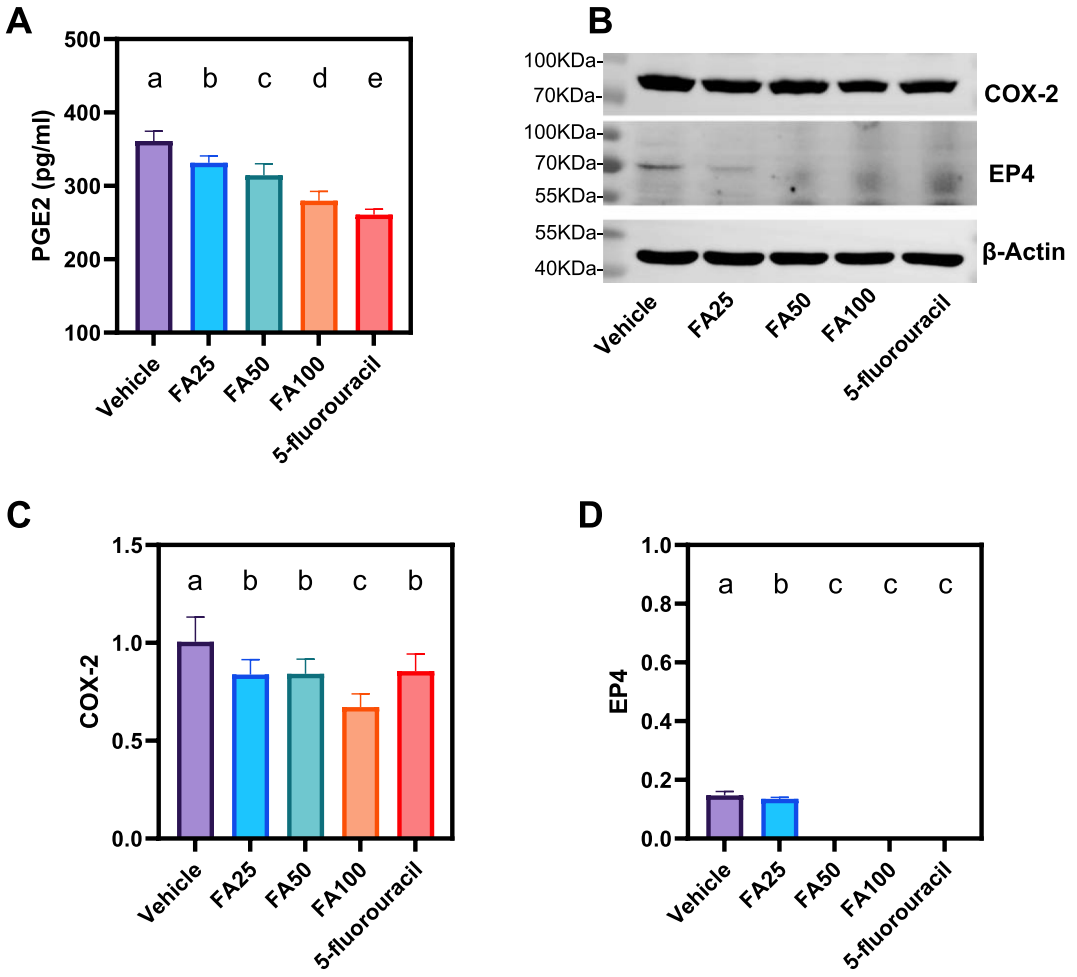

Fig. 6. FAs downregulate the expressions of COX-2/PGE2/EP4 related proteins. (A) The expression of PGE2 in serum ($p < 0.001$, one-way ANOVA, n = 30), (B) COX-2 and EP4 were assayed by western blotting, β-Actin served as a loading control, and the expressions of (C) COX-2 and (D) EP4 ($p < 0.001$, one-way ANOVA, n = 4 independent experiments) in tumor tissue. Means not sharing any lowercase letters are significantly different by the SNK test at the 5% level of significance.

biological responses. FA molecular docking and dynamic simulations showed that hydrogen bonds, van der Waals forces, and hydrophobic interactions were responsible for binding of FA to COX-2 and EP4. Saturation, high affinity, specificity, and reversibility are features of this type of binding. The predicted binding sites for FA to COX-2 and EP4 were identical to the proteins' natural binding pockets, and the binding affinity was less than −7 kcal/mol, indicating the binding energy was mainly reliable.

The binding energy of 5-fluorouracil to COX-2 and EP4 were weak and the binding site did not match the binding pocket of the protein with natural ligands. In silico simulation and WB findings both suggest that FA can directly affect COX-2 and EP4, which would reduce their protein activity or decrease their protein expression and exert antitumor effects though the COX-2/PGE2/EP4 pathway. Although 5-fluorouracil decreased serum PGE2 levels and the expression of COX-2 and EP4 in tumors, the assumption that 5-

fluorouracil inhibits the COX-2/PGE2/EP4 pathway to reduce tumor growth was not supported by molecular docking simulation. This finding does not conflict with the fact that 5-fluorouracil exerts anticancer effect though additional mechanisms or pharmacological actions (thymidylate synthase inhibitors).

In clinical practice, the traditional antitumor medications used as positive controls, such as 5-fluorouracil, paclitaxel, and other chemotherapeutic medications, are almost exclusively administered intravenously. Drugs based on oral 5-fluorouracil have large inter- and intra-patient variability in plasma 5-fluorouracil concentration, which contributes to treatment failure [45]. To use as few mice as possible to achieve stable experimental results, we chose the most clinically applicable administration method to ensure the reliability of 5-fluorouracil as a positive control. Therefore, we used a small number of mice in the fulvic acid group and divided them into three groups for evaluation based on the dose administered. Owing to limitations in purification technology, FAs, a key component of traditional Chinese medicine, cannot be administered intravenously. Therefore, the primary objective of this study was to confirm antitumor effect of FAs without detailing the administration strategy or drug metabolism. Additionally, oral administration rather than intravenous administration or development as a functional excipient for FAs may have better application prospects, based on the current research status and viewpoint of the development of new antitumor drugs [33,46].

The in vivo studies reported in this paper showed that FA significantly inhibited tumor growth compared to the vehicle group. The concentration of PGE2 in the vehicle group was the highest, and the concentration of PGE2 in the serum of the FA groups decreased, based on the ELISA analysis. WB results showed low expression of COX-2 and EP4 in the FA groups. An investigation of the effects of FA on homocysteine-induced COX-2 expression in human monocytes showed that FA attenuated or inhibited COX-2 expression [47]. Our findings on the effect of FA on COX-2 are in line with the findings of the paper.

As the positive control group, 5-fluorouracil showed significant antitumor effect. Although 5-fluorouracil also reduced COX-2 and EP4 expression in tumor tissues, computer simulations indicated that it did not act by binding to COX-2 and EP4, which did not conflict with the pharmacological effects of 5-fluorouracil (a thymidylate synthase inhibitor). In silico results showed that FA competitively binds to the active site of COX-2 to exert an enzyme inhibitory effect and reduce the production of PGE2. Competitively binding PGE2 to the active site of EP4 can reduce the activation of EP4. Overall, the expression of COX-2/PGE2/EP4-related proteins decreased. When the FA concentration is low, the active site binding of the COX-2 protein in the tumor tissue is not saturated, and the synthesis of the enzyme product PGE2 is first reduced, leading to a significant reduction in the activation of downstream EP4. When the concentration of PGE2 decreased to a critical value, EP4 could not be activated because of the low concentration of PGE2 itself or because of the inhibition of EP4 by FA. Although the overall activity and expression of detectable COX-2 in tumor tissues decreased, there was no significant difference, and the activity and expression of EP4 were significantly decreased. As the drug concentration of FAs continues to increase, more active sites of the COX-2 protein are competitively inhibited and gradually saturated. At this time, the detectable activity and expression of COX-2 in tumor tissues were significantly reduced compared to those at low doses, and the production of PGE2 was further reduced. However, since its concentration falls below the activation threshold of ep4, or the active center of EP4 has been saturated and inhibited by FA, its expression cannot be detected.

Regarding the COX-2/PGE2 pathway, it is necessary to discuss cancer-related inflammation (CRI) [48]. CRI play important roles in the development and occurrence and of cancer. In addition, another study reported that the aromatic structure of FA can protect zebrafish larvae from inflammation at 5 and 50 mg C/L [49]. Another study has reported the use of FA to prevent chronic inflammatory diseases [50]. The anti-inflammatory action of humic substances can inhibit the release of inflammation-related cytokines, adhesion molecules, oxidants, and components of the complement system [51]. The inhibition of cyclooxygenase and prostaglandin synthesis by FA may be another mechanism underlying its anti-inflammatory effects. Here, we also raised another question, namely, whether FA can exert antipyretic and analgesic effects through COX-2/PGE2, which will be discussed in a future study. Khan et al. reported a combination study of thymoquinone and peat-sourced FA nanoemulgels, which may promote the dissolution and absorption of drugs and reduce toxic or side effects [52]. This innovative and easily clinically implementable idea provides important clues for future research. If FA is developed as a delivery system for chemotherapeutic medications with antitumor effects, subsequent studies should focus on whether it enhances the antitumor effects of such drugs or reduce drug resistance.

The current study has several limitations. First, FAs are natural products obtained from coal or plants. The characteristics of the products produced from various coal types, geographical locations, and extraction techniques vary significantly. This study has not yet addressed the pharmacokinetics and pharmacodynamics of FAs in depth; it is merely a preliminary investigation of the acute toxicity and anti-NSCLC effects. In addition, the results of this study are insufficient for direct clinical use because FA's pharmacological mechanism studies and the current purification methods do not permit the use of this substance as a first-line antitumor treatment. Second, the finding that FA inhibits tumor growth though the COX-2/PGE2/EP4 pathway was only achieved using the results of molecular docking and molecular dynamics simulation in silico. In vivo animal studies have provided indirect support rather than direct evidence for this claim, showing that FA can reduce COX-2 and EP4 expression in the tumor tissues of A549 tumor-bearing mice. The purpose of this article was to assess the expressions of COX-2, EP4, and PGE2 in vivo, so only WB and ELISA techniques were conducted. However, as organisms are complex, whether FA can regulate the COX-2/PGE2/EP4 axis through other targets requires further experimental proof. To gain further insight into the influence of FA on the activity and expression of COX-2 and EP4, we plan to conduct further research using quantitative polymerase chain reaction (qPCR), flow cytometry, and enzyme activity assays that involve FA, COX-2 and EP4 in various cell lines.

5. Conclusions

Natural FAs do not exhibit developmental toxicity. We characterized the anti-NSCLC activity of FAs. The mechanism of action is mediated by the inhibition of COX-2 and EP4 expression and PGE2 production through the COX-2/PGE2/EP4 axis.

Declarations

Ethics statement

All procedures were conducted in accordance with the National Research Council's Guide for the Care and Use of Laboratory Animals and were approved by the Laboratory Animal Ethical and Welfare Committee of Shanxi Bethune Hospital at the Shanxi Academy of Medical Science (SBQDL-2022-067).

Author contributions

Pengfei Xin conceived and designed the experiments; Wrote the paper.
Shirui Wang, Xin Xu performed the experiments and data collection; Analyzed and interpreted the data.
Qingmei Liu conceived and designed the experiments.
Caifeng Zhang contributed reagents, materials, analysis tools.

Data availability statement

The data presented in this study are available on request from the corresponding authors.

Funding

This study was supported by the Fundamental Research Program of Shanxi Province (202203021221240), Program of State Key Laboratory of Quantum Optics and Quantum Optics Devices, Shanxi University (KF202105), Fund for Shanxi Bethune Hospital "Beacon Project" Talent Training (2022FH18), and Fund for Shanxi "1331 Project" Collaborative Innovation Center.

Declaration of competing interest

The authors declare that they have no known competing financial interests or personal relationships that could have appeared to influence the work reported in this paper.

Acknowledgment

The authors thank all our colleagues who provided assistance during the current study and Elsevier's English language editing service for this paper.

Appendix A. Supplementary data

Supplementary data to this article can be found online at https://doi.org/10.1016/j.heliyon.2023.e17080.

References

[1] R.L. Siegel, K.D. Miller, H.E. Fuchs, A. Jemal, Cancer statistics, 2022, CA A Cancer J. Clin. 72 (1) (2022) 7–33, https://doi.org/10.3322/caac.21708.
[2] R. Zheng, S. Zhang, H. Zeng, S. Wang, K. Sun, R. Chen, L. Li, W. Wei, J. He, Cancer incidence and mortality in China, 2016, J. Nat. Canc. Cent. 2 (1) (2022) 1–9, https://doi.org/10.1016/j.jncc.2022.02.002.
[3] T. Yang, Y. Xiong, Y. Zeng, Y. Wang, J. Zeng, J. Liu, S. Xu, L.S. Li, Current status of immunotherapy for non-small cell lung cancer, Front. Pharmacol. 13 (2022), 989461, https://doi.org/10.3389/fphar.2022.989461.
[4] E.N. Imyanitov, A.G. Iyevleva, E.V. Levchenko, Molecular testing and targeted therapy for non-small cell lung cancer: current status and perspectives, Crit. Rev. Oncol. Hematol. 157 (2021), 103194, https://doi.org/10.1016/j.critrevonc.2020.103194.
[5] M. Reck, D. Rodriguez-Abreu, A.G. Robinson, R. Hui, T. Csoszi, A. Fulop, M. Gottfried, N. Peled, A. Tafreshi, S. Cuffe, M. O'Brien, S. Rao, K. Hotta, T.A. Leal, J. W. Riess, E. Jensen, B. Zhao, M.C. Pietanza, J.R. Brahmer, Five-year outcomes with pembrolizumab versus chemotherapy for metastatic non-small-cell lung cancer with PD-L1 tumor proportion score >/= 50, J. Clin. Oncol. 39 (21) (2021) 2339–2349, https://doi.org/10.1200/JCO.21.00174.
[6] O. Abughanimeh, A. Kaur, B. El Osta, A.K. Ganti, Novel targeted therapies for advanced non-small lung cancer, Semin. Oncol. (2022), https://doi.org/10.1053/j.seminoncol.2022.03.003.
[7] N. Hashemi Goradel, M. Najafi, E. Salehi, B. Farhood, K. Mortezaee, Cyclooxygenase-2 in cancer: a review, J. Cell. Physiol. 234 (5) (2019) 5683–5699, https://doi.org/10.1002/jcp.27411.
[8] H. Moon, A.C. White, A.D. Borowsky, New insights into the functions of Cox-2 in skin and esophageal malignancies, Exp. Mol. Med. 52 (4) (2020) 538–547, https://doi.org/10.1038/s12276-020-0412-2.
[9] S.Y. Ye, J.Y. Li, T.H. Li, Y.X. Song, J.X. Sun, X.W. Chen, J.H. Zhao, Y. Li, Z.H. Wu, P. Gao, X.Z. Huang, The efficacy and safety of celecoxib in addition to standard cancer therapy: a systematic review and meta-analysis of randomized controlled trials, Curr. Oncol. 29 (9) (2022) 6137–6153, https://doi.org/10.3390/curroncol29090482.
[10] V. Ganduri, K. Rajasekaran, S. Duraiyarasan, M.A. Adefuye, N. Manjunatha, Colorectal carcinoma, cyclooxygenases, and COX inhibitors, Cureus 14 (8) (2022), e28579, https://doi.org/10.7759/cureus.28579.
[11] Y.Q. Xu, X. Long, M. Han, M.Q. Huang, J.F. Lu, X.D. Sun, W. Han, Clinical benefit of COX-2 inhibitors in the adjuvant chemotherapy of advanced non-small cell lung cancer: a systematic review and meta-analysis, World J. Clin. Cases 9 (3) (2021) 581–601, https://doi.org/10.12998/wjcc.v9.i3.581.

[12] K. Jin, C. Qian, J. Lin, B. Liu, Cyclooxygenase-2-Prostaglandin E2 pathway: a key player in tumor-associated immune cells, Front. Oncol. 13 (2023), 1099811, https://doi.org/10.3389/fonc.2023.1099811.

[13] S. Sharma, S.C. Yang, L. Zhu, K. Reckamp, B. Gardner, F. Baratelli, M. Huang, R.K. Batra, S.M. Dubinett, Tumor cyclooxygenase-2/prostaglandin E2-dependent promotion of FOXP3 expression and CD4+ CD25+ T regulatory cell activities in lung cancer, Cancer Res. 65 (12) (2005) 5211–5220, https://doi.org/10.1158/0008-5472.CAN-05-0141.

[14] S. Hazra, S.M. Dubinett, Ciglitazone mediates COX-2 dependent suppression of PGE2 in human non-small cell lung cancer cells, Prostaglandins Leukot. Essent. Fatty Acids 77 (1) (2007) 51–58, https://doi.org/10.1016/j.plefa.2007.05.006.

[15] L. Bazzani, S. Donnini, A. Giachetti, G. Christofori, M. Ziche, PGE2 mediates EGFR internalization and nuclear translocation via caveolin endocytosis promoting its transcriptional activity and proliferation in human NSCLC cells, Oncotarget 9 (19) (2018) 14939–14958, https://doi.org/10.18632/oncotarget.24499.

[16] S. Sarvepalli, V. Parvathaneni, G. Chauhan, S.K. Shukla, V. Gupta, Inhaled indomethacin-loaded liposomes as potential therapeutics against non-small cell lung cancer (NSCLC), Pharm. Res. (N. Y.) 39 (11) (2022) 2801–2815, https://doi.org/10.1007/s11095-022-03392-x.

[17] G. O'Callaghan, A. Houston, Prostaglandin E2 and the EP receptors in malignancy: possible therapeutic targets? Br. J. Pharmacol. 172 (22) (2015) 5239–5250, https://doi.org/10.1111/bph.13331.

[18] N. Bhooshan, P.N. Staats, A.M. Fulton, J.L. Feliciano, M.J. Edelman, Prostaglandin E Receptor EP4 expression, survival and pattern of recurrence in locally advanced NSCLC, Lung Cancer 101 (2016) 88–91, https://doi.org/10.1016/j.lungcan.2016.09.011.

[19] K. Osawa, M. Umemura, R. Nakakaji, R. Tanaka, R.M. Islam, A. Nagasako, T. Fujita, U. Yokoyama, T. Koizumi, K. Mitsudo, Y. Ishikawa, Prostaglandin E(2) receptor EP4 regulates cell migration through Orai1, Cancer Sci. 111 (1) (2020) 160–174, https://doi.org/10.1111/cas.14247.

[20] J. Wu, Q. Tang, X. Ren, F. Zheng, C. He, X. Chai, L. Li, S.S. Hann, Reciprocal interaction of HOTAIR and SP1 together enhance the ability of Xiaoji decoction and gefitinib to inhibit EP4 expression, J. Ethnopharmacol. 237 (2019) 128–140, https://doi.org/10.1016/j.jep.2019.03.027.

[21] Y. Chen, Q. Tang, Q. Xiao, L. Yang, S.S. Hann, Targeting EP4 downstream c-Jun through ERK1/2-mediated reduction of DNMT1 reveals novel mechanism of solamargine-inhibited growth of lung cancer cells, J. Cell Mol. Med. 21 (2) (2017) 222–233, https://doi.org/10.1111/jcmm.12958.

[22] S. Iwasa, T. Koyama, M. Nishino, S. Kondo, K. Sudo, K. Yonemori, T. Yoshida, K. Tamura, T. Shimizu, Y. Fujiwara, S. Kitano, A. Shimomura, J. Sato, F. Yokoyama, H. Iida, M. Kondo, N. Yamamoto, First-in-human study of ONO-4578, an antagonist of prostaglandin E2 receptor 4, alone and with nivolumab in solid tumors, Cancer Sci. (2022), https://doi.org/10.1111/cas.15574.

[23] C. Pi, P. Jing, B. Li, Y. Feng, L. Xu, K. Xie, T. Huang, X. Xu, H. Gu, J. Fang, Reversing PD-1 resistance in B16F10 cells and recovering tumour immunity using a COX2 inhibitor, Cancers 14 (17) (2022), https://doi.org/10.3390/cancers14174134.

[24] V. Karpisheh, J. Fakkari Afjadi, M. Nabi Afjadi, M.S. Haeri, T.S. Abdpoor Sough, S. Heydarzadeh Asl, M. Edalati, F. Atyabi, A. Masjedi, F. Hajizadeh, S. Izadi, F. S. Mirzazadeh Tekie, M. Hajiramezanali, M. Sojoodi, F. Jadidi-Niaragh, Inhibition of HIF-1alpha/EP4 axis by hyaluronate-trimethyl chitosan-SPION nanoparticles markedly suppresses the growth and development of cancer cells, Int. J. Biol. Macromol. 167 (2021) 1006–1019, https://doi.org/10.1016/j.ijbiomac.2020.11.056.

[25] A.G. Zavarzina, N.N. Danchenko, V.V. Demin, Z.S. Artemyeva, B.M. Kogut, Humic substances: hypotheses and reality (a review), Eurasian Soil Sci. 54 (12) (2021) 1826–1854, https://doi.org/10.1134/S1064229321120164.

[26] B.A. de Melo, F.L. Motta, M.H. Santana, Humic acids: structural properties and multiple functionalities for novel technological developments, Mater. Sci. Eng. C Mater. Biol. Appl. 62 (2016) 967–974, https://doi.org/10.1016/j.msec.2015.12.001.

[27] Z.H. Miao, K. Li, P.Y. Liu, Z. Li, H. Yang, Q. Zhao, M. Chang, Q. Yang, L. Zhen, C.Y. Xu, Natural humic-acid-based phototheranostic agent, Adv. Healthc. Mater. 7 (7) (2018), e1701202, https://doi.org/10.1002/adhm.201701202.

[28] M. Calisir, A. Akpinar, A.C. Talmac, A. Lektemur Alpan, O.F. Goze, Humic acid enhances wound healing in the rat palate, Evid. Based Complem. Alter. Med. 2018 (2018), 1783513, https://doi.org/10.1155/2018/1783513.

[29] F. Samiee-Rad, S.F. Hosseini Sedighi, A. Taherkhani, N. Gheibi, Evaluation of healing effects of poultice containing 0.5% fulvic acid on male white-male rats with skin ulcer, J. Cutan. Aesthetic Surg. 15 (1) (2022) 40–47, https://doi.org/10.4103/JCAS.JCAS_215_20.

[30] D.C. Socol, Clinical review of humic acid as an antiviral: leadup to translational applications in clinical humeomics, Front. Pharmacol. 13 (2022), 1018904, https://doi.org/10.3389/fphar.2022.1018904.

[31] Z. Wang, H. Zhang, Y. Qin, W. Dai, B. Li, M. Zhang, Angiogenic effects of low molecular weight organic acids present in fulvic acids of different sources, Nat. Prod. Res. 35 (24) (2021) 6153–6157, https://doi.org/10.1080/14786419.2020.1830399.

[32] C. Dai, X. Xiao, Y. Yuan, G. Sharma, S. Tang, A comprehensive toxicological assessment of fulvic acid, Evid. Based Complem. Alter. Med. 2020 (2020), 8899244, https://doi.org/10.1155/2020/8899244.

[33] K. Gnananath, K.S. Nataraj, B.G. Rao, K.P. Kumar, M.H. Mahnashi, M.K. Anwer, A. Umar, Z. Iqbal, M.A. Mirza, Exploration of fulvic acid as a functional excipient in line with the regulatory requirement, Environ. Res. 187 (2020), 109642, https://doi.org/10.1016/j.envres.2020.109642.

[34] W.S. Huang, J.T. Yang, C.C. Lu, S.F. Chang, C.N. Chen, Y.P. Su, K.C. Lee, Fulvic acid attenuates resistin-induced adhesion of HCT-116 colorectal cancer cells to endothelial cells, Int. J. Mol. Sci. 16 (12) (2015) 29370–29382, https://doi.org/10.3390/ijms161226174.

[35] R. Jayasooriya, M.G. Dilshara, C.H. Kang, S. Lee, Y.H. Choi, Y.K. Jeong, G.Y. Kim, Fulvic acid promotes extracellular anti-cancer mediators from RAW 264.7 cells, causing to cancer cell death in vitro, Int. Immunopharm. 36 (2016) 241–248, https://doi.org/10.1016/j.intimp.2016.04.029.

[36] P. Kavaliauskas, F.S. Opazo, W. Acevedo, R. Petraitiene, B. Grybaite, K. Anusevicius, V. Mickevicius, S. Belyakov, V. Petraitis, Synthesis, biological activity, and molecular modelling studies of naphthoquinone derivatives as promising anticancer candidates targeting COX-2, Pharmaceuticals 15 (5) (2022), https://doi.org/10.3390/ph15050541.

[37] D.E. Pires, T.L. Blundell, D.B. Ascher, pkCSM: predicting small-molecule pharmacokinetic and toxicity properties using graph-based signatures, J. Med. Chem. 58 (9) (2015) 4066–4072, https://doi.org/10.1021/acs.jmedchem.5b00104.

[38] J. Eberhardt, D. Santos-Martins, A.F. Tillack, S. Forli, AutoDock Vina 1.2.0: new docking methods, expanded force field, and Python bindings, J. Chem. Inf. Model. 61 (8) (2021) 3891–3898, https://doi.org/10.1021/acs.jcim.1c00203.

[39] B. Zhang, T. Jiang, X. She, S. Shen, S. Wang, J. Deng, W. Shi, H. Mei, Y. Hu, Z. Pang, X. Jiang, Fibrin degradation by rtPA enhances the delivery of nanotherapeutics to A549 tumors in nude mice, Biomaterials 96 (2016) 63–71, https://doi.org/10.1016/j.biomaterials.2016.04.015.

[40] T.S. Murbach, R. Glavits, J.R. Endres, A.E. Clewell, G. Hirka, A. Vertesi, E. Beres, I. Pasics Szakonyine, A toxicological evaluation of a fulvic and humic acids preparation, Toxicol Rep 7 (2020) 1242–1254, https://doi.org/10.1016/j.toxrep.2020.08.030.

[41] A.V. Vucskits, I. Hullar, A. Bersenyi, E. Andrasofszky, M. Kulcsar, J. Szabo, Effect of fulvic and humic acids on performance, immune response and thyroid function in rats, J. Anim. Physiol. Anim. Nutr. 94 (6) (2010) 721–728, https://doi.org/10.1111/j.1439-0396.2010.01023.x.

[42] M. Swat, I. Rybicka, A. Gliszczynska-Swiglo, Characterization of fulvic acid beverages by mineral profile and antioxidant capacity, Foods 8 (12) (2019), https://doi.org/10.3390/foods8120605.

[43] J. Yu, D. Qi, J. Li, Design, synthesis and applications of responsive macrocycles, Commun. Chem. 3 (1) (2020) 189, https://doi.org/10.1038/s42004-020-00438-2.

[44] G. Bitencourt-Ferreira, M. Veit-Acosta, W.F. de Azevedo Jr., Hydrogen bonds in protein-ligand complexes, Methods Mol. Biol. 2053 (2019) 93–107, https://doi.org/10.1007/978-1-4939-9752-7_7.

[45] S. Kobuchi, M. Tsuda, M. Okamura, T. Nakamura, Y. Ito, A pharmacokinetic-pharmacodynamic model predicts uracil-tegafur effect on tumor shrinkage and myelosuppression in a colorectal cancer rat model, Anticancer Res. 43 (3) (2023) 1121–1130, https://doi.org/10.21873/anticanres.16257.

[46] S.J. Nass, M.L. Rothenberg, R. Pentz, H. Hricak, A. Abernethy, K. Anderson, A.W. Gee, R.D. Harvey, S. Piantadosi, M.M. Bertagnolli, D. Schrag, R.L. Schilsky, Accelerating anticancer drug development - opportunities and trade-offs, Nat. Rev. Clin. Oncol. 15 (12) (2018) 777–786, https://doi.org/10.1038/s41571-018-0102-3.

[47] S.J. Chien, T.C. Chen, H.C. Kuo, C.N. Chen, S.F. Chang, Fulvic acid attenuates homocysteine-induced cyclooxygenase-2 expression in human monocytes, BMC Compl. Alternative Med. 15 (2015) 61, https://doi.org/10.1186/s12906-015-0583-x.

[48] A. Mantovani, P. Allavena, A. Sica, F. Balkwill, Cancer-related inflammation, Nature 454 (7203) (2008) 436–444, https://doi.org/10.1038/nature07205.

[49] T. Lieke, C.E.W. Steinberg, T. Meinelt, K. Knopf, W. Kloas, Modification of the chemically induced inflammation assay reveals the Janus face of a phenol rich fulvic acid, Sci. Rep. 12 (1) (2022) 5886, https://doi.org/10.1038/s41598-022-09782-w.
[50] J. Winkler, S. Ghosh, Therapeutic potential of fulvic acid in chronic inflammatory diseases and diabetes, J. Diabetes Res. 2018 (2018), 5391014, https://doi.org/10.1155/2018/5391014.
[51] C.E. van Rensburg, The antiinflammatory properties of humic substances: a mini review, Phytother Res. 29 (6) (2015) 791–795, https://doi.org/10.1002/ptr.5319.
[52] R. Khan, M.A. Mirza, M. Aqil, N. Hassan, F. Zakir, M.J.J. Ansari, Z. Iqbal, A pharmaco-technical investigation of thymoquinone and peat-sourced fulvic acid nanoemulgel: a combination therapy, Gels 8 (11) (2022), https://doi.org/10.3390/gels8110733.